Layer-by-Layer Assembly of Rectifying Junctions in and on Metal Nanowires†

Nina I. Kovtyukhova,*,‡,§ Benjamin R. Martin,‡ Jeremiah K. N. Mbindyo,‡ Peter A. Smith,|| Baharak Razavi,|| Theresa S. Mayer,|| and Thomas E. Mallouk*,‡

Department of Chemistry, 152 Davey Laboratory, The Pennsylvania State University, University Park, Pennsylvania 16802, and Institute of Surface Chemistry, N.A.S.U., 17, General Naumov Street, 03680 Kyiv, Ukraine, and Department of Electrical Engineering, The Pennsylvania State University, University Park, Pennsylvania 16802

Received: March 7, 2001; In Final Form: June 23, 2001

Alumina membranes containing 200 nm diameter pores were replicated electrochemically with metals (Au and Ag) to make free-standing nanowires several microns in length. Wet layer-by-layer assembly of nanoparticle (TiO_2 or ZnO)/polymer thin films was carried out in the membrane between electrodeposition steps to give nanowires that contained rectifying junctions. Concentric structures with similar properties were prepared by first coating the membrane walls with multilayer films, and then growing nanowires inside the resulting tubules, or by growing films on the exposed surface of the nanowires after dissolution of the membrane. The $I-V$ characteristics of nanowires prepared by either technique show current rectifying behavior. The electronic properties of Au(MEA)/$(ZnO/PSS)_{19}$ZnO/Ag (MEA = mercaptoethylamine) devices indicate that rectification is determined by charge injection at the metal/ZnO/PSS-film interface rather than by a tunneling mechanism. In the case of Ag$(TiO_2/PSS)_9TiO_2$/Au devices, switching behavior and hysteresis that could not be described by Schottky or Fowler−Nordheim characteristics was found. The combined replication/layer-by-layer synthetic approach allows one to control both the geometry and the chemical composition of diode nanowire devices.

Introduction

As the scaling of lithographically made electronic circuits approaches practical and fundamental limits, alternative fabrication approaches, based on the chemical assembly of nanoscale and molecular devices, are being researched with increasing interest. Since the pioneering work of Murray and co-workers on thin film polymer diodes,[1] there have been numerous reports of molecule- and polymer-based devices that can function as rectifiers, transistors, and switches.[2] One of the best recognized barriers to using these devices in real applications is the wiring problem: how one makes the appropriate connections between nanoscale and molecular devices, and how input/output wires are connected to the larger (lithographic) scale of conventional wiring. Because of this problem, most proposed circuits use two-terminal rather than three-terminal devices, and some elaborate logic circuits based on molecular diodes have been proposed.[3] Nanoscale crossbar arrays that contain bistable memory elements have recently been made,[4] but again it is acknowledged that current rectification will be needed at each crossing point in order to isolate individual memory elements from each other.

Our approach to the wiring problem has been to use well-established membrane replication methods[5] to make nanowires of precisely controlled length, diameter, and connection chemistry along their length.[6] The wires are made by electrochemically growing a series of metals in the cylindrical pores of an alumina or polycarbonate membrane. By controlling the charge passed in each plating step, one can make a precisely defined series of "stripes" along the nanowires. These stripes can subsequently be derivatized with appropriate monolayer-forming molecules. Interactions between complementary molecules (hydrophobic, hydrophilic, anionic, cationic, single-stranded DNA) on specific stripes programs the adhesion of nanowires to each other and to complementary patterns on planar surfaces. For example, one can make nanowires that assemble deterministically into cross- or T-shaped pairs, or into more complex shapes.[7]

This technique, and other assembly methods such as microfluidic alignment,[8] hold some promise for constructing logic gates and crosspoint memories from sub-lithographic components. However, to date nanowires that incorporate the two-terminal nonlinear devices needed for these circuits—diodes and switches—have not been available. On the other hand, wet layer-by-layer assembly has been shown to be an experimentally simple but powerful route to functional nanoscale devices with thickness controlled to nanometer precision.[9] This method involves the spontaneous adsorption of preformed colloidal particles and/or organic macromolecules as monolayers.[10−21] Many research efforts have now been focused on making multilayer nanoparticle/polymer films with structure- and sequence-dependent electronic functions. These include Coulomb blockade devices,[22] rectifying diodes,[18−20,23] electroluminescent devices,[24] photon harvesting and charge separation assemblies,[25a] and multicomponent energy/electron-transfer cascades that mimic some of the functions of natural photosynthetic assemblies.[25b] Because it is an adsorption technique, the layer-by-layer assembly method can be equally applied to planar or curved surfaces.

In this paper we describe a combined synthetic route, using template replication and layer-by-layer assembly together, to nanowire diodes. Two different diode structures have been realized: (i) semiconductor/polymer films sandwiched between two segments of a nanowire, i.e., an "in-wire" diode and (ii) semiconductor/polymer films that cover the walls of a nanowire, such that contacting the wire with another crossing wire gives a rectifying junction. The synthesis of the first structure involves

† Part of the special issue "Royce W. Murray Festschrift".
‡ Department of Chemistry.
§ Institute of Surface Chemistry.
|| Department of Electrical Engineering.

10.1021/jp010867z CCC: $20.00
Published on Web 08/14/2001

the assembly of a multilayer TiO_2 (or ZnO)/polymer film on top of a metal nanowire inside the pores of an alumina or polycarbonate membrane, followed by electrochemical or chemical growth of a second metal segment. Our previous work using planar substrates has shown that multilayer TiO_2/polymer and ZnO/polymer films can be easily grown on suitably primed (Au or Pt) and bare (Ag) metal surfaces, and that these films act as diodes when contacted with an appropriate top metal.[17,18,23a]

Two different strategies were used to make the second structure, in which the semiconductor/polymer film covers the walls of a metal nanowire. The first one is based on the concept of sequential tubular synthesis, which was introduced by Martin for fabrication of rod-shaped concentric nanocomposite particles.[26] This method exploits surface chemistry of the membrane pore walls. We extend this approach to layer-by-layer assembly of semiconductor/polymer tubule shells stuck to the walls, inside which metal nanowire core is electrochemically or chemically grown. Recently we found that densely packed TiO_2/polymer films could be prepared on planar Al substrates bearing thin surface layer of native oxide.[17]

The second strategy exploits reactivity of metal rod surface, and involves layer-by-layer growth of the semiconductor/polymer shell around the metal nanowire core. This method follows from our recent experiments that show that rod-shaped nanoparticles can be used as a substrate for layer-by-layer assembly of smooth, conformal films of insulating organic polyelectrolytes.[27]

Experimental Section

Materials. Whatman Anopore disks of 200 nm pore diameter (Al_2O_3-membranes) were used for templates for nanowire growth. Cracks in the membrane resulting from handing were sealed using cement (Bond 527). Electrochemical metal deposition was carried out using commercially available gold (Technic Orotemp 24), platinum (Technic TP), and silver (Technic Silver 1025) plating solutions. Titanium tetraisopropoxide [$Ti(O\text{-}^iPr)_4$], zinc acetate dihydrate [$Zn(ac)_2$], lithium hydroxide monohydrate, mercaptoethylamine hydrochloride (MEA), aqueous (20 wt %) poly(sodium 4-styrenesulfonate) (PSS), ethyltriethoxysilane, and chlorotrimethylsilane were purchased from Aldrich. *N*-Octadecyltrichlorosilane (OTS) was purchased from Gelest, Inc. All the reagents were used without further purification. All other chemicals were reagent grade and obtained from commercial sources.

TiO_2 colloids were prepared as follows. [$Ti(O\text{-}^iPr)_4$] was dissolved in cooled, stirred 2-methoxyethanol. The solution was stirred until it became slightly yellow, after which another portion of 2-methoxyethanol containing HCl was added. The molar ratio of the components in the solution was [$Ti(O\text{-}^iPr)_4$]:HCl:2-methoxyethanol = 1:0.2:20. This solution was diluted with water to adjust the TiO_2 concentration to 1% and was allowed to age for 3 weeks. The resulting opalescent sol was subjected to the rotary evaporation at 60 °C to give a shiny xerogel powder containing 75% (w/w) titania. This xerogel was used as a precursor for preparing stock aqueous sols with TiO_2 concentration and pH varying in the range of 2.3−3.5 wt % and 1.5−3, respectively. These sols were stable over periods of several weeks. Powder X-ray diffraction (XRD) of the titania xerogel gave an average size of the colloidal anatase crystals of about 6 nm.[17] Transmission electron microscope (TEM) images of the stock TiO_2 sol showed 4−10 nm diameter particles.

ZnO colloids were synthesized according to the method of Spanhel and Anderson.[28] Briefly, $Zn(ac)_2$ (11 g) and 0.5 l of anhydrous ethanol were placed in a distillation apparatus and boiled at 82° C for 3 h. At the end of the procedure, 0.2 l of a hygroscopic solution was obtained. This solution was diluted with ethanol to adjust the Zn^{2+} concentration to 0.1 M. Then 3 g (0.14 mol) of $LiOH\cdot H_2O$ powder was added, and the mixture was sonicated to dissolve the powder. Next, the solution was concentrated by rotary evaporation to yield a viscous sol (∼2.0 M), which was stable for a period of several months. A stock solution was prepared for film synthesis by diluting (1:10) the ZnO sol with anhydrous ethanol. TEM images of the stock ZnO sol showed particles of 3−5 nm in diameter.

The emmeraldine base (EB) form of polyaniline (PAN) was prepared as described by Chiang and MacDiarmid.[29] A dark blue solution of PAN in dimethyl formamide (0.015wt %) was used as a stock solution for film synthesis.

Synthesis of Nanowire Diodes. *Nanowires Containing in-Wire Diode Junctions.* A four step process used to prepare these nanowires consisted of electroplating the bottom metal electrode, layer-by-layer assembly of the multilayer film, electroplating the top metal electrode, and removing the template. Metal electrodes were grown electrochemically inside the 200 nm diameter pores of alumina membranes as described previously.[6a] Briefly, the membrane (3.14 cm^2, containing approximately 9 × 10^8 pores/cm^2) was pretreated by evaporating ∼150 nm of silver on its branched side. To fill the pores completely on this side, 1 C of silver was electroplated onto the evaporated silver. These Ag "plugs" were used as foundations onto which long (30 μm) sacrificial Ag base rods were electroplated (galvanostatically at 300 mA/cm^2) to fill the branched part of the pores. Upon this base, the bottom Au metal electrode was grown (galvanostatically at 0.55 mA/cm^2). Silver bottom electrodes were prepared by electroplating more silver (0.5−3 μm) on the top of the gold segment (galvanostatically, 0.55 mA/cm^2). Control experiments on planar metal substrates showed that no priming procedure was necessary for the silver bottom electrode, whereas a priming monolayer of MEA should precede the deposition of multilayer TiO_2/polymer films on gold. This was achieved by a 24 h adsorption of MEA onto the exposed tips of the metal nanowires from a 5% ethanolic solution. The nanoparticle/polymer multilayer film was grown by successively immersing the membrane in the TiO_2 and polymer stock solutions for 15−30 min. Each adsorption step was followed by removal of excess reagents by soaking the membrane in several portions of an appropriate solvent (0.01 M aqueous HCl for TiO_2, water for PSS, and DMF for PAN) for 30 min, and then drying the membrane in an Ar stream. Finally a top electrode (typically Au) of the desired length was electroplated over the TiO_2/polymer multilayer (galvanostatically at 0.55 mA/cm^2). The Ag base electrode was removed by immersion in 6 M nitric acid, and the alumina membrane was dissolved in 0.5−1 M NaOH. Control experiments showed that multilayer TiO_2/polymer films grown on planar Ag or Au/MEA substrates were not removed by NaOH. The resulting suspension of nanowire diodes was then repeatedly centrifuged and resuspended in water.

In most of these experiments, the Al_2O_3-membrane pore walls were made hydrophobic by treatment with alkylchlorosilane derivatives in order to control wetting by the plating solution and electrodeposited metal. Treatment with OTS, for example, was performed as follows. The membrane was soaked in absolute ethanol for1 h and dried over drierite in a vacuum for 2 h, after which it was immediately immersed in an OTS solution in CCl_4+octane (volume ratio CCl_4:octane:OTS = 3:7:0.1; t = 8 °C) for 15 h. The membrane was then successively

soaked in 3 portions of anhydrous cyclohexane for 1 h and heated at ~100 °C in air for 2 h. When the membrane was derivatized in this manner, ethanol was added to the plating solutions (10 vol %) so the solutions could wet the pore walls.

Diode Devices in Which the Semiconductor/Polymer Film Covers the walls of a Nanowire. Two strategies used to prepare these diode devices consisted of 1. layer-by-layer synthesis of TiO_2/polymer tubules on the alumina pore walls, followed by electrochemical or chemical deposition of metal inside the tubules.

An alumina membrane was immersed in the TiO_2 stock solution for 15 min, placed in a suction filtering unit and washed with two 15 mL portions of aqueous HCl (pH ~ 2) under vacuum. The membrane was then dried in an Ar stream and immersed in an aqueous 1 wt % PSS solution (pH 3.4) for 15 min. The same washing procedure was done using deionized water, and the membrane was dried in an Ar stream. Vacuum filtering of the washings allowed fast removal of excess reagents from the pores, thus preventing their blocking; drying the membrane in the Ar stream provided for convective transport of the nanoparticle sol and polymer solutions into the pores. Ten layer TiO_2/PSS films were grown on the pore walls by repeating these steps.

To grow Au nanowires inside the TiO_2/PSS tubules, the plating conditions needed to be significantly adjusted. When electroplating was done under the same conditions used for underivatized alumina membranes, no solid nanowires of the desired (several micron) length were found. Instead, breaks inside the metal cores were observed along the tubule length, resulting in the recovery of short (0.3−1 mm) gold rods covered with TiO_2/PSS films when the membranes were dissolved. We tentatively explain this by stronger adsorption of Au ions (and a greater tendency to form Au nuclei) on the inner surface of TiO_2/PSS tubules and/or higher electrical conductivity of tubule walls compared to underivatized alumina. Both factors could promote the growth of gold metal along the walls; these metal segments could close the pores leaving voids between segments. To overcome this problem, gold was electroplated in these tubules potentiostatically at −800 mV vs saturated calomel electrode (SCE). This resulted in slower metal growth compared to the galvanostatic method, but gave continuous wires of the desired length.

The chemical deposition of Au inside the TiO_2/PSS tubules was performed by a slight modification of the method developed by Menon and Martin for electroless Au plating in pores of polycarbonate membranes.[5c] The tubule was first activated by adsorption of $SnCl_3^-$ ions onto the positively charged TiO_2-terminated inner surface (5 min immersion of the $Al_2O_3/(TiO_2/PSS)_9TiO_2$ membrane in a solution of $SnCl_2 \cdot 2H_2O$ in methanol: H_2O = 3:2 (0.5 wt %, pH~2) followed by washing with MeOH in the filtering unit under vacuum, and drying in an Ar stream. Adsorption of $SnCl_3^-$ ions was evidenced by the change in membrane color from white to yellow. The membrane was then immersed (for 2 min) in 0.025 M aqueous silver ammoniate (pH~11), washed with water, and dried in an Ar stream. The membrane was then placed in an Au plating bath (85 mL of an aqueous solution containing 0.008 M $Na_3Au(SO_3)_2$, 0.127 M Na_2SO_3, and 0.625 M formaldehyde) for 110 h. To deposit gold selectively insice the membrane, the bath temperature was kept in the range of 2−6 °C. Finally, these Au-filled $Al_2O_3/(TiO_2/PSS)_9TiO_2$ membranes were dissolved in 1M NaOH.

2. Layer-by-layer deposition of (TiO_2 or ZnO)/PSS films on the surface of the metal nanowires was performed in two ways.

(a) Eight micron long gold rods were grown electrochemically as described above and transferred to aqueous solution by dissolving the evaporated silver backing and electroplated silver "plugs" (6 M nitric acid) and the alumina membrane (1 M NaOH). The water was replaced by ethanol, and the gold surface was derivatized with MEA (21 h adsorption from a 1.5 wt % ethanolic solution). Layer-by-layer assembly of multilayer ZnO/PSS film on the primed surface of the nanowire was carried out as follows. Ethanolic ZnO and aqueous PSS (1 wt %, pH ~ 7) were alternately added to the concentrated (by centrifuging) suspension of nanowires in the appropriate solvent. Each 5 min adsorption cycle was followed by a centrifugation/washing cycle with three portions of the appropriate solvent, which was then replaced by the solvent used in the next adsorption step. In this way Au nanowires covered by an $MEA/(ZnO/PSS)_{19}ZnO$ film were prepared.

(b) Eight micron long gold rods with a 0.5 mm silver top segment were grown electrochemically inside an alumina membrane. The Ag-covered face of the metal-filled membrane was cemented to a glass slide, and the membrane was dissolved (in 1 M NaOH) leaving the Au/Ag nanowire array attached to the silver base. This Ag/Au/Ag "brush" was subjected to the layer-by-layer deposition procedure for multilayer TiO_2/PSS films. Briefly, nanowire surface was primed with MEA (21 h adsorption from a 1.5 wt % ethanolic solution). Onto this positively charged $Au(NH_2)$ surface, a 10 layer PSS/TiO_2 film was grown by alternately immersing (for 5 min) the "brush" in solutions of the components. Aqueous 1 wt % PSS solution (pH 3.4) was used; postadsorption washings were done with aqueous HCl (pH ~ 2) and deionized water for TiO_2 and PSS, respectively. Importantly, during the film growth and washing, the "brush" was always kept wet to prevent the silver base from deforming and breaking during drying. Finally, the Ag parts of the "brush" were dissolved in 1 M HNO_3 releasing the Au-$(MEA)/(PSS/TiO_2)_{10}$ nanowires into the colloidal suspension.

Characterization. Transmission electron microscope (TEM) images were obtained with a JEOL 1200 EXII at 80 kV accelerating voltage and 60 μA filament current. Optical microscope (OM) images were recorded using an Olympus BX60M. Transmission infrared spectra were recorded with a Perkin-Elmer 1600 series FTIR.

Current−voltage characteristics of the nanowire diodes were measured in air at ambient temperature. Nanowire integration into the circuit was achieved by AC electrofluidic alignment, which positioned individual nanowires between lithographically prepared contact pads.[31]

Results and Discussion

Diode Devices in Which the Semiconductor/Polymer Film Covers the Walls of a Nanowire. *Multilayer TiO_2/Polymer Tubules Self-Assembled on the Pore Walls.* TEM images of $(TiO_2/PSS)_9TiO_2$ tubules grown on the alumina membrane pore walls followed by membrane dissolution are shown in Figure 1. The tubules as prepared are typically unbroken with an average outside diameter of about 300 nm (the diameter of the pores) and length ranging from 5 mm to 15 mm. The tubule ends are always open and their length is less than the thickness of the template membrane (~70 μm). This implies that the tubules are broken during the membrane dissolution or subsequent handling. A higher resolution TEM image (Figure 1b) shows uniform tubule walls of densely packed TiO_2 particles of ~5 nm diameter (the particle diameter in the stock TiO_2 solution). The thickness of the walls increases with the number of adsorption cycles and can be estimated as 40 nm for a ten-layer TiO_2/PSS tubule. This value is consistent with the

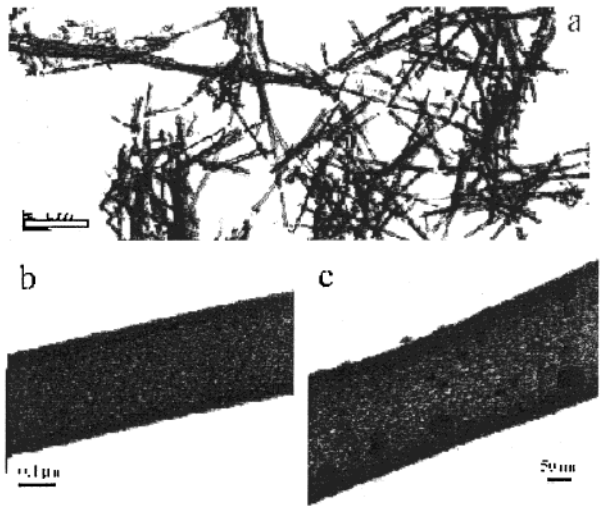

Figure 1. (a,b) Low and high-resolution TEM images of $(TiO_2/PSS)_9TiO_2$ tubules prepared by layer-by-layer self-assembly in 200 nm diameter alumina membrane pores followed by dissolution of the membrane. (c) $(TiO_2/PSS)_9TiO_2$ tubule activated for electroless Au deposition by successive adsorption of $SnCl_3^-$ ions and $Ag(NH_3)_2^+$.

ellipsometric thickness (37 nm) of 10 layer TiO_2/PSS films grown on planar substrates. The outer surface of the tubules is quite smooth and its shape appears to follow the pore walls. One can see round-ended branches on some of the tubule walls, which reflect the structure of the alumina membrane pores in their branched part. These observations suggest strong adsorption of the first TiO_2 nanoparticle layer, which gives rise to densely packed tubule walls. Our previous study showed that TiO_2 colloidal particles formed a well-packed single particle layer on a planar Al/Al_2O_3 substrate.[17]

The FTIR spectrum (not shown) of an alumina membrane subjected to ten TiO_2/PSS adsorption cycles shows new band maxima at 2935, 2841, 2347, 1637, 1497, 1450, 1412, and 1127 cm^{-1}. These peaks are observed in the spectrum of PSS, and confirms the presence of PSS in the membrane. Apparently the adsorption of PSS polyanions onto the positively charged (at pH < 6) TiO_2-terminated surface is driven by electrostatic interactions.

Gold Deposition within the $(TiO_2/PSS)_9TiO_2$ Tubules. Gold deposition could be accomplished either chemically or electrochemically. In the case of electroless deposition, the tubules were first primed by adsorption of $SnCl_3^-$ ions and then treated with $Ag(NH_3)_2^+$. It is known that treatment of Sn-sensitized surfaces with $Ag(NH_3)_2^+$ leads to reduction of the silver cations and formation of Ag aggregates, which provide a nucleation site for the electroless deposition of Au.[30] Indeed, evenly distributed 5−50 nm diameter metallic nanoparticles are clearly seen by TEM on the inner surface of the TiO_2/PSS tubules (Figure 1c).

A typical TEM image of Au-filled $(TiO_2/PSS)_9TiO_2$ tubules (Figure 2a) shows solid metal rods with walls bearing a thin nanoparticle film. The film looks featureless and rather smooth. Its roughness, which is determined by the roughness of the pore walls, is comparable to the average size of the TiO_2 colloidal particles, ∼5 nm. The Au-filled TiO_2/PSS tubules appeared to break within 5−50 nm of the ends of the gold rods. This leaves the rod ends accessible for further derivatization by wet chemical or vapor phase techniques. The length of the coated nanowires prepared this way was in the range of 3−5 μm for electrochemical plating and 2−12 μm for electroless plating.

Layer-by-Layer Assembly on the Surface of Template-Grown Au-Rods. An important advantage of this strategy, compared

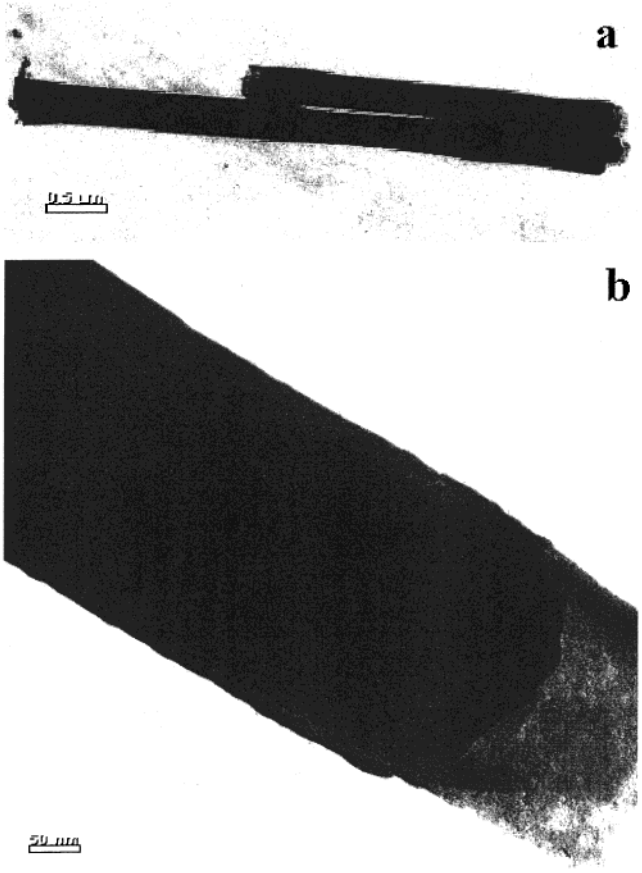

Figure 2. (a,b) Low and high resolution TEM images of Au nanowires grown electrochemically inside $(TiO_2/PSS)_9TiO_2$ tubules. The tubule-coated nanowires were released from the silver backing and the membrane by etching in aqueous HNO_3 and NaOH, respectively.

to the one described above, is its applicability to a wide range of nanoparticle/polymer films which might be destroyed under the conditions used to dissolve the template membrane. This method also allows one to prepare nanowires with ends accessible for further functionalization, by starting with a sacrificial metal (e.g., Ag or Cu) at the tips of the wires.

Figure 3 shows TEM images of gold nanowires that were electrochemically grown and released from the alumina membrane, and then subjected to 20 ZnO/PSS adsorption cycles. One can see that the nanoparticle film completely covers the walls and ends of the nanowires. The film thickness is approximately 40 nm, which is less than expected, since on planar Au substrates the average thickness per ZnO/PSS adsorption cycle is 3 nm per ZnO/PSS. Although the film is relatively uniform, its surface is rather rough; in contrast, similar films grown on planar Au are smooth by AFM. It is possible that aggregates are formed from suspended ZnO particles and PSS chains in solution (due to incomplete removal of reagents during the washing−centrifuging stage) and that these aggregates precipitate on the nanowire surface.

An alternate way to deposit these films is to use a nanowire array attached to a silver base. Recently we successfully used such a "brush" for preparing polyelectrolyte-coated gold nanowires.[27] Figure 3d shows a TEM image of an $Au(PSS/TiO_2)_{10}$ nanowire isolated from such a "brush" after dissolution of the Ag backing. Dissolving the sacrificial Ag layer on the ends of the Au nanowires leaves them uncovered, but unfortunately, some uncovered areas of the nanowire walls are also observed. It is interesting to note that the same film growth procedure on a planar Au-substrate resulted in high quality 10 layer PSS/

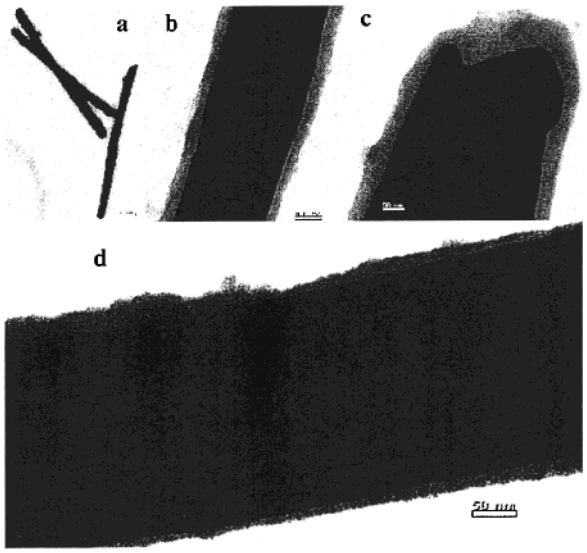

Figure 3. (a−c) Low and high-resolution TEM images of Au nanowires that were grown in alumina membranes, then released with HNO_3 and NaOH and subjected to 20 ZnO/PSS adsorption cycles. One can see the nanoparticle film completely covering the walls (b) and ends (c) of the rods (scale bar 50 nm). A high resolution image of a $Au(NH_2)(PSS/TiO_2)_{10}$ nanowire prepared by the "brush" is shown in (d).

TiO_2 film with a thickness of ∼37 nm. An experiment with nitric acid (used for dissolving the Ag backing) showed that this film was not significantly changed. The poor quality of the $(PSS/TiO_2)_{10}$ film on the nanowire walls probably results from the fact that some nanowires in the "brush" can contact each other, thereby preventing the access of nanoparticles and polymer chains to the surface.

Nanowires Containing in-Wire Diode Junctions. TEM images of gold nanowires grown in alumina membranes show that the two ends of the wire differ in their topography: the base end is bulging and rounded, while the growing end has an apparent hollow in the middle (cup-shaped). This difference can be understood in terms of adsorption of metal ions on the wall, and preferential wetting of the polar alumina surface by the reduced metal. It was recently shown that Au(III) complexes are taken up by hydrous aluminum oxide by formation of Au−O−Al bonds. These adsorbed Au(III) ions were spontaneously reduced to the metallic state without added reducing agents.[32] If the same reaction takes place in alumina membranes, it will promote metal growth on the wall leading to a cup-shaped tip.

To probe the topography of multilayer TiO_2/polymer films sandwiched between Au and Ag nanowire segments, we prepared $Au/(TiO_2/PAN)_6/Ag$ junctions and dissolved the top Ag segments in the nitric acid. The remaining Au wires with $(TiO_2/PAN)_6$ films deposited at their ends were imaged by TEM (Figure 4). Control experiments showed that the ellipsometric thickness of a multilayer TiO_2/PAN film grown on a planar Au/MEA substrate did not decrease after immersion in 6 M HNO_3 for 30 min, indicating that the film is stable in the medium used to etch away the Ag segment. A TEM image of an $Au/(TiO_2/PAN)_6$ nanowire (Figure 4a) shows the profile of the cup-shaped tip. After focusing the electron beam on this tip for some time (typically tens of seconds), a nanoparticle film appears at the tip (Figure 4b), perhaps because of beam-induced melting of the metal. Comparing Figure 4a,b, one can see that the upper contour line of the film is very close to that of the cup-shaped tip before melting. Apparently, the multilayer film grows on both the cup bottom and cup walls and thus retains the cup shape after the thin walls have melted. This explanation is

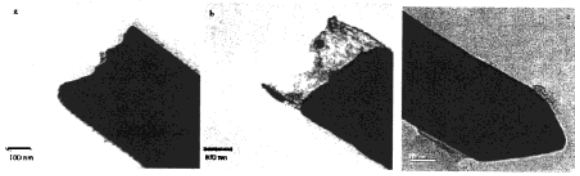

Figure 4. (a,b) TEM images of an $Au/(TiO_2/PAN)_6/Ag$ nanowire taken after dissolving the top Ag segment with HNO_3: (a) the image taken immediately after focusing the electron beam; (b) the image taken after focusing the electron beam on the nanowire tip for tens of seconds. (c) TEM image of the top-end of an Au nanowire prepared using an alumina membrane that had been treated with OTS.

consistent with observed film height of ∼100 nm (Figure 4b), which approximates the cup depth rather than the $(TiO_2/PAN)_6$ film thickness. The ellipsometric thickness of a $(TiO_2/PAN)_6$ film on a planar Au(MEA) substrate is about 10 nm.

The tip shape (which may influence the uniformity and continuity of nanoparticle junctions between metal segments) can be altered by passivation of the pore walls by alkylsilane derivatives, such as OTS, ethyltriethoxysilane or chlorotrimethylsilane. Transmission IR spectra of an alumina membrane treated with OTS showed new intense bands at 2960, 2920, 2850 cm^{-1} (ν C−H), 1470 cm^{-1} (δ C−H), and 1100 cm^{-1} (ν Si−O). Membranes derivatized this way were hydrophobic, confirming the adsorption of OTS on the pore walls and faces of the membrane. TEM images of Au nanowires grown from OTS-treated alumina showed a tendency for the previously cup-shaped end to become pointed (Figure 4c). Thus, the derivatization of the wall of the membrane to some extent allows one to smooth the surface of the rod ends.

Figure 5 shows the reaction scheme for in-wire layer-by-layer assembly and dissolution of the template and silver backing. The optical micrograph in Figure 5 shows one of the suspended $Au/Ag/(TiO_2/PSS)_{10}TiO_2/Au$ nanowires, in which a silver "stripe" can be clearly seen between two gold ends. A TEM image of such a nanowire recorded within the first several seconds, as with the $Au/(TiO_2/PAN)_6$ rods, shows no visible signs of a metal/film/metal heterojunction. However, after focusing the electron beam on this nanowire for several seconds, a break appears due to beam-induced metal melting in the neighborhood of the Au/film/Ag junction. Particles of 5−10 nm diameter, which adhere to both metal ends, are observed. Apparently, the TiO_2 nanoparticles are present between the two electroplated metal segments. The optical and TEM data confirm that a multilayer TiO_2/polymer film can be assembled layer by layer on the tip of a metal rod in the membrane, and that this film does not prevent electroplating the second metal segment on the top of the film.

Interestingly, for $Au/Ag/(TiO_2/PSS)_{10}TiO_2/Au$ nanowires grown in OTS-treated alumina membranes, a very thin (<5 nm) film can be seen on the walls of the bottom metal segments. This suggests that the OTS SAM deposited on the pore walls adheres to the nanowire surface after the membrane is dissolved away. In principle, this effect could be used to prepare ultrathin insulating films around the metal nanowires.

Electrical Properties. Optical micrographs of test structures used to characterize the electrical properties of in-rod devices and concentric nanowire/nanoparticle devices are shown in Figure 6a,b, respectively.

A typical $I-V$ curve for the $Au(NH_2)/(ZnO/PSS)_{19}ZnO/Ag$ structure (Figure 7) with the ZnO/PSS film deposited on the walls of an Au nanowire reveals the expected current rectifying behavior with turn-on potentials at ∼ −1.25 V and ∼2.02 V for forward (Ag "−") and reverse (Ag "+") biases, respectively.

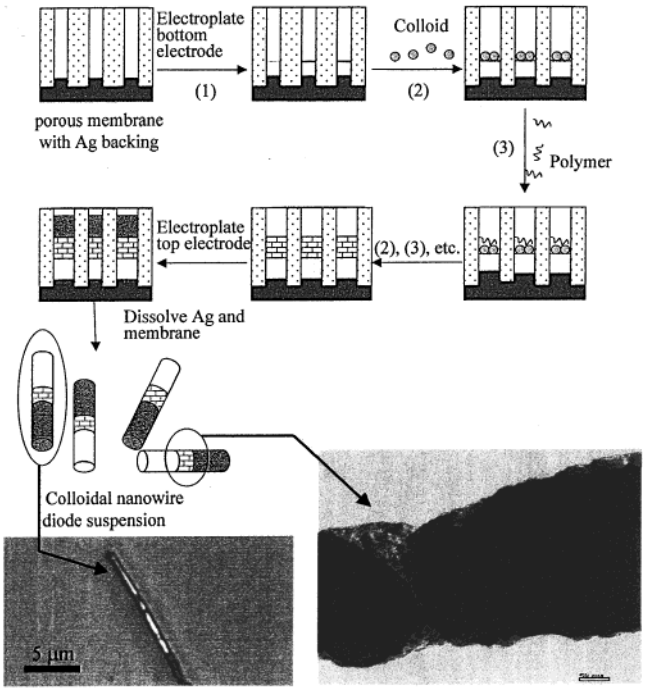

Figure 5. Layer by layer adsorption scheme for the preparation of in-wire diode junctions. The optical micrograph at the lower left shows an Au/Ag/$(TiO_2/PSS)_{10}TiO_2$/Au nanowire prepared in an OTS-treated alumina membrane. The two Au ends appear darker than the central silver stripe. One Au segment was made longer than the other so that the junction could be easily identified. The nanoparticle junction is at the bottom end of the silver stripe in the image. A high resolutionTEM image of a similar nanowire (lower right) was taken after focusing the electron beam for several seconds. Beam-induced metal melting in the neighborhood of the Au/film/Ag junction reveals 5−10 nm diameter particles that adhere to both metal ends.

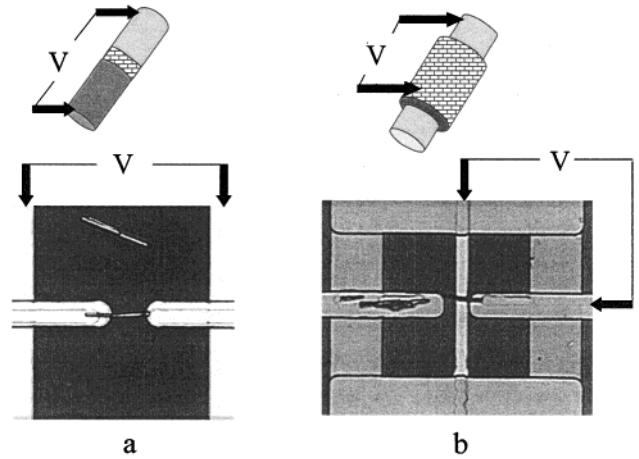

Figure 6. Optical micrographs of test structures for measuring the electrical properties of (a) in-wire devices and (b) devices in which the semiconductor/polymer film covers the walls of the nanowire. In (a), a Au/Ag$(TiO_2/PSS)_{10}TiO_2$/Au nanowire was aligned between two gold pads and 175 nm thick gold contacts were evaporated on the top of the ends of the nanowire. In (b), an Au nanowire bearing a ZnO/PSS multilayer film on the walls was aligned between two gold pads. Electrical contact was made by evaporation of 30 nm thick Ag stripe at right angles to the wire, followed by evaporation of 175 nm thick gold contacts on the ends.

The difference between numerical values of the turn-on potentials is in reasonable agreement with the difference between the work functions of Ag (∼4.6 eV) and Au (∼5.3 eV). The operating voltage is also close to the ZnO band gap (3.28 eV, as estimated from the UV−visible spectrum of starting ZnO sol), and both branches of this curve can be successfully linearized using the Schottky equation ($\ln(I) \propto V$). These observations suggest that rectification is determined by charge injection at the metal/ZnO/PSS-film interface. However, we cannot eliminate a tunneling mechanism, since the $I-V$ curve also shows quite satisfactory linearity in Fowler−Nordheim $\{\ln(I/V^2) \propto 1/V\}$ coordinates.

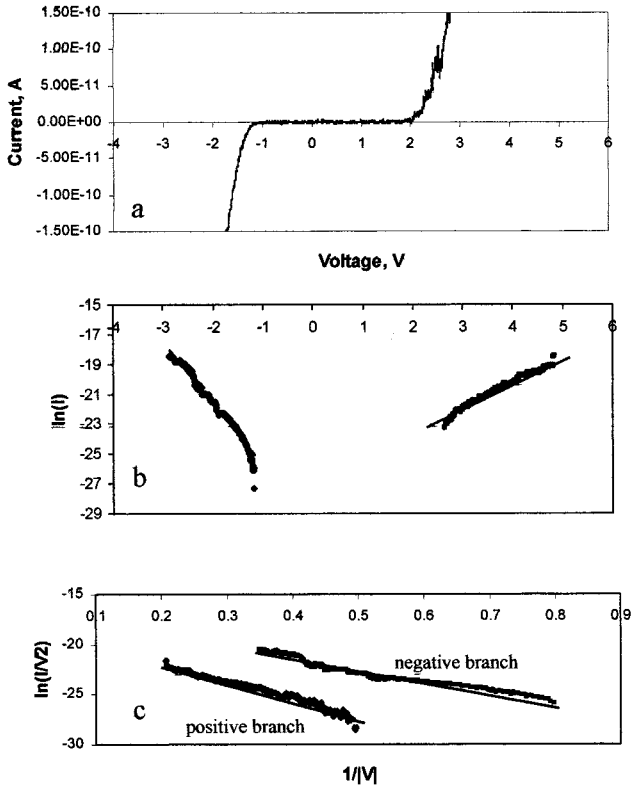

Figure 7. $I-V$ characteristics of a Au(MEA)/$(ZnO/PSS)_{19}$ZnO/Ag nanowire. The data are plotted in Schottky and Fowler−Nordheim coordinates in (b) and (c).

Typical $I-V$ characteristics of Au/$(TiO_2/PSS)_9TiO_2$/Ag structures prepared as in-rod devices (the TiO_2/PSS film is sandwiched between bottom silver and top gold segments of the nanowire), and devices in which the TiO_2/PSS film covers the Au nanowire walls, are shown in Figure 8a, curves 1and 2, respectively. For comparison purposes, the $I-V$ characteristic of the same structure grown on a planar Au substrate and top-contacted with evaporated Ag is also shown (Figure 8a, curve 3). (This planar device was prepared by the layer-by-layer self-assembly of a ten-layer PSS/TiO_2 film on an Au-substrate primed with MEA). One can see that all three curves are rather similar in shape, showing an abrupt current increase at turn-on potentials.

Although for all three devices, the differences between the numerical values of the "forward" and "reverse" turn-on potentials are close (∼ 0.35−0.5 eV), they are less than that expected for the difference in work functions between Ag (∼4.6 eV) and Au (∼5.3 eV). These values also differ for different devices prepared the same way. The charge transport in these TiO_2/PSS thin-film devices cannot be described by either the Schottky or Fowler−Nordheim equations. In some cases the $I-V$ curve shape suggests breakdown characteristic of insulators, but such "breakdowns" are quite reproducible in 4−6 successive voltage sweeps, and this is not usually observed for breakdown in insulators.

The comparison between the $I-V$ curves of the Au/$(TiO_2/PSS)_9TiO_2$/Ag structures and bare Au/TiO_2/Ag (Figure 8a.4)

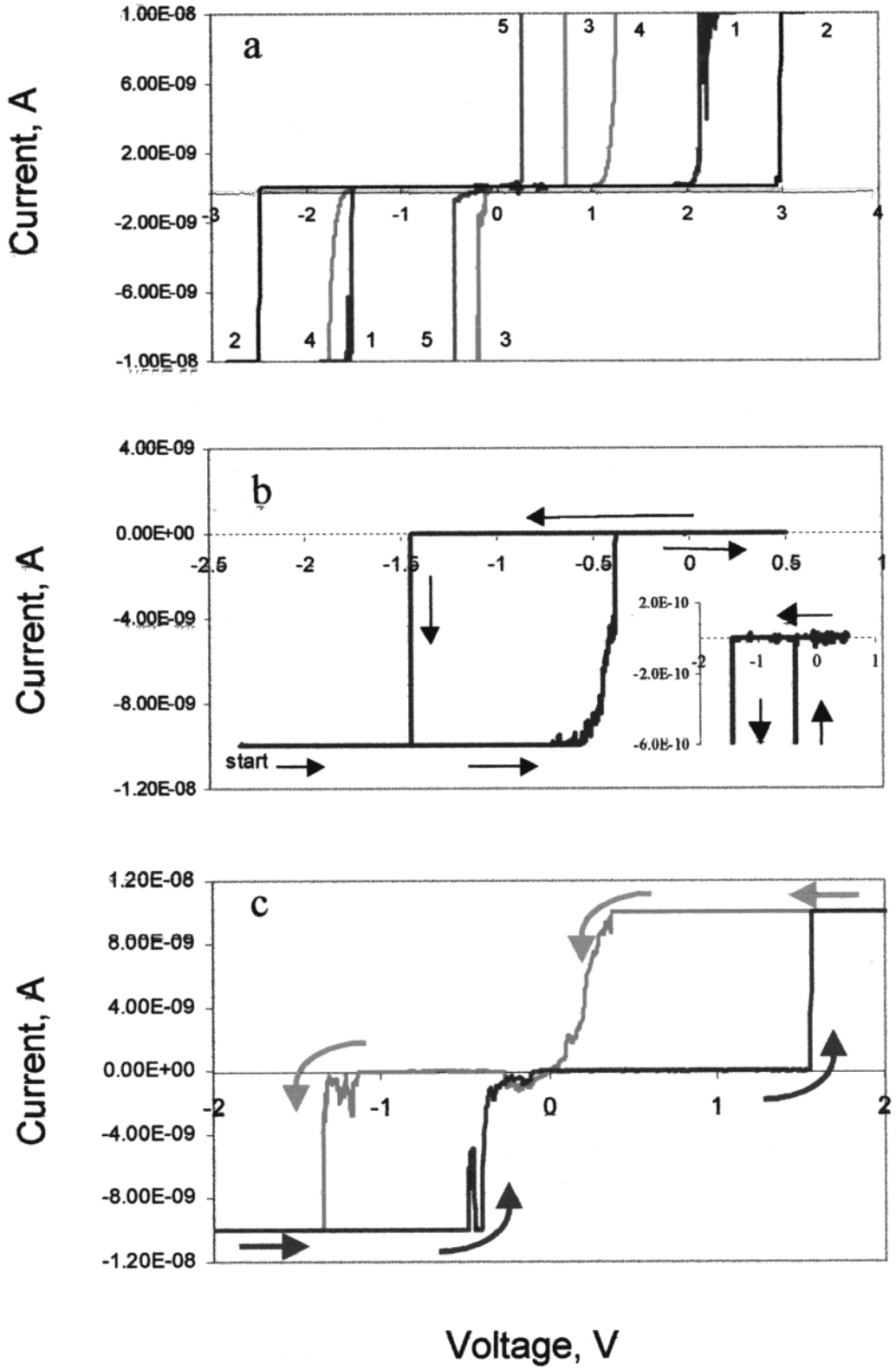

Figure 8. $I-V$ curves for nanowire and planar $Ag(TiO_2/PSS)_9TiO_2/Au$ devices and planar Ag/TiO2/Au and Ag/PSS/Au devices: (a) (1) An in-wire $Ag(TiO_2/PSS)_9TiO_2/Au$ device; (2) a concentric device containing Au inside a $(TiO_2/PSS)_9TiO_2$ tubule, contacted as in Figure 7b with Ag; (3) a planar $Au/(TiO_2/PSS)_9TiO_2$ device top contacted with evaporated Ag, device area $\sim 1\ \mu m^2$; (4) a planar $Au/TiO_2/Ag$ device, area $\sim 1\ \mu m^2$; and (5) a planar Au/PSS/Ag device, area $\sim 1\ \mu m^2$. All $I-V$ curves were measured in two sweeps starting from 0 V. (b) A planar $Au/(TiO_2/PSS)_9TiO_2$ device top contacted with evaporated Ag, device area $\sim 1\ \mu m^2$, showing the persistence of the hysteresis loop when the scan is reversed at intermediate voltage. The scan shown was initiated at -2.5 V and reversed at $+0.5$ V. The inset curve, with an expanded current scale, shows that the conductance is very low in the reverse sweep. (c) An in-wire $Ag(TiO_2/PSS)_9TiO_2/Au$ device measured in single sweeps starting from (1) $+3$V and (2) -3V. The current is limited at 1×10^{-8} A by the test circuit.

and Au/PSS/Ag (Figure 8a.5) suggests that the PSS plays a role in the abrupt transition from a nonconducting to a conducting state. The $I-V$ curve of bare Au/PSS/Ag device shows breakdown at relatively low potentials ($\sim +0.26$ V and -0.46 V) for both forward and reverse bias modes. It is intersting to note that no "breakdowns" were observed when PAN or PAH

was used instead of PSS in planar Au(TiO_2/polymer)Ag devices. Among all the polymers investigated by us (PAN, PAH, PAA, PDDA, and PEI) PSS provides the most regular growth of multilayer TiO_2/polymer films, but its electrical properties do not allow us to consider PSS as the best candidate for diode preparation.

All the $I-V$ curves shown in Figure 8a were obtained in one positive and one negative sweep, each starting after a long hold time (2−5 min) at zero volts. If instead the scan is initiated at high negative or positive bias, there is an interesting hysteresis in the curves. The $I-V$ curves of a planar device, shown in Figure 8b, were obtained by starting at a high negative bias and reversing the sweep at +0.5 V. The device turns "off" at approximately −0.4 V and does not turn "on" again until the voltage is swept back beyond the negative breakdown threshold of −1.4 V. Similar behavior (with opposite polarity) was observed when the $I-V$ curves were recorded starting at high positive bias.

The same kind of hysteresis loops are found with crossbar and in-wire devices, as shown in Figure 8c. In this example, the scans were reversed at high potential (beyond the positive and negative breakdown voltages). Again, the switching from the low to high conductance state is consistent with a type of breakdown—perhaps via charging of the TiO_2 particle or the polymer—that abruptly increases the conductivity of the device. The conductivity returns to near zero at an intermediate potential, and then increases again at the breakdown potential in the other direction. Although the electrical properties of these devices are not yet understood, we note that the hysteresis shown in Figures 8b,c might be useful in memory devices if persistent high- and low-conductivity states can be attained in a range of intermediate voltages.

Conclusions

We have shown that it is possible to couple the template synthesis of metal nanowires with layer-by-layer assembly of polymer/colloid films, to realize simple devices that act as rectifiers. The availability of in-wire and concentric rectifying films opens up the possibility of constructing logic gates and crosspoint devices by means of electrofluidic or chemically driven nanowire assembly. While the device characteristics shown here are poor by the standards of the semiconductor industry, it is important to note that only primitive layer sequences (simple polymer/colloid repeats) were used. It should be possible to make more structured films in which asymmetry is built in (e.g., with electron- and hole-conducting segments) to allow better rectification ratios, lower turn-on voltages, and more complex device functions. Preliminary data show that it is also possible to make in-wire junctions with single layers of self-assembling monolayers. This opens the door to using a wider variety of molecular electronic switches and other devices in self-assembling circuits. These possibilities will be explored in future work.

Acknowledgment. We thank the DARPA Moletronics Program and the Office of Naval Research for support of this work.

References and Notes

(1) (a) Abruña, H. d.; Denisevich, P.; Umana, M.; Meyer, T. J.; Murray, R. W. *J. Am. Chem. Soc.* **1981**, *103*, 1. (b) Denisevich, P.; Willman, K. W.; Murray, R. W. *J. Am. Chem. Soc.* **1981**, *103*, 4727. (c) Pickup, P. G.; Kutner, W.; Leidner, C. R.; Murray, R. W. *J. Am. Chem. Soc.* **1984**, *106*, 1991.

(2) (a) Kittlesen, G. P.; White, H. S.; Wrighton, M. S. *J. Am. Chem. Soc.* **1985**, *107*, 7373. (b) Kittlesen, G. P.; Wrighton, M. S. *J. Mol. Electron.* **1986**, *2*, 23. (c) Friend, R.; Burroughes, J.; Shimoda, T. *Phys. World* **1999**, *12*, 35. (d) Roman, L. S.; Berggren, M.; Inganas, O. *Appl. Phys. Lett.* **1999**, *75*, 3557. (e) Chen, J.; Reed, M. A.; Rawlett, A. M.; Tour, J. M. *Science* **1999**, *286*, 1550. (f) Metzger, R. M.; Chen, B.; Höpfner, U.; Lakshmikantham, M. V.; Vuillaume, D.; Kawai, T.; Wu, X.; Thachibana, H.; Hughes, T. V.; Sakurai, H.; Baldwin, J. W.; Hosch, C.; Cava, M. P.; Brehmer, L.; Ashwell, G. J. *J. Am. Chem. Soc.* **1997**, *119*, 10455.

(3) Ellenbogen, J. C.; Love, J. C., *Proc. IEEE* **2000**, *88*, 386.

(4) (a) Rueckes, T.; Kim, K.; Joselevich, E.; Tseng, G. Y.; Cheung, C.-L.; Lieber, C. M. *Science* **2000**, *289*, 94. (b) Collier, C. P.; Wong, E. W.; Belohradsky, M.; Raymo, F. M.; Stoddart, J. F.; Kuekes, P. J.; Williams, R. S.; Heath, J. R. *Science* **1999**, *285*, 391. (c) Collier, C. P.; Mattersteig, G.; Wong, E. W.; Luo, Y.; Beverly, K.; Sampaio, J.; Raymo, F.; Stoddart, J. F.; Heath, J. R. *Science* **2000**, *289*, 1172.

(5) (a) Al-Mawlawi, D.; Liu, C. Z.; Moskovits, M. *J. Mater. Res.* **1994**, *9*, 1014. (b) Nishizava, M.; Menon, V. P.; Martin, C. R. *Science* **1995**, *268*, 700. (c) Menon, V.; Martin, C. R. *Anal. Chem.* **1995**, *67*, 1920. (d) Martin, C. R. *Chem. Mater.* **1996**, *8*, 1739. (e) Wang, L.;Yu-Zhang, K.; Metrot, A.; Bonhomme, P.; Troyon, M. *Thin Solid Films* **1996**, *288*, 86. (f) Martin, C. R.; Parthasarathy, R. V. *Adv. Mater.* **1995**, *7*, 487. (g) Lakshmi, B. B.; Dorhout, P. K.; Martin, C. R. *Chem. Mater.* **1997**, *9*, 857.

(6) (a) Martin, B. R.; Dermody, D. J.; Reiss, B. D.; Fang, M.; Lyon, L. A.; Natan, M. J.; Mallouk, T. E. *Adv. Mater.* **1999**, *11*, 1021. (b) Mbindyo, J. K. N.; Reiss, B. D.; Martin, B. R.; Keating, C. D.; Natan, M. J.; Mallouk, T. E. *Adv. Mater.*, **2001**, *13*, 249.

(7) Reiss, B. D.; Mbindyo, J. N. K.; Martin, B. R.; Nicewarner, S. R.; Mallouk, T. E.; Natan, M. J.; Keating, C. D. *Mater. Res. Soc. Symp. Proc.* **2001**. In press.

(8) Huang, Y.; Duan, X.; Wei, Q.; Lieber, C. M. *Science* **2001**, *291*, 630.

(9) (a) Fendler, J. H.; Meldrum, F. *Adv. Mater.* **1995,** *7*, 607. (b) Mallouk, T. E.; Kim, H.-N.; Ollivier, P. J.; Keller, S. W. In *Comprehensive Supramolecular Chemistry*; Alberti, G., Bein, T., Eds.; Elsevier Science, Oxford, UK, 1996; Vol. 7, p 189.

(10) Iler, R. K *J. Colloid Interface Sci.* **1966**, *21*, 569.

(11) Decher, G. *Science* **1997**, *277*, 1232.

(12) Keller, S. W.; Kim, H.-N.; Mallouk, T. E. *J. Am. Chem. Soc.* **1994**, *116*, 8817.

(13) Colvin, V. L.; Golstein, A. N.; Alivisatos, A. P. *J. Am. Chem. Soc.* **1992**, *114*, 5221.

(14) Fendler, J. *Chem. Mater.* **1996**, *8*, 1616−1624.

(15) Ollivier, P. J.; Kovtyukhova, N. I.; Keller, S. W.; Mallouk, T. E. *Chem. Commun.* **1998**, 1563.

(16) Fang, M.; Kim, H.-N.; Saupe, G. B.; Miwa, T.; Fujishima, A.; Mallouk, T. E. *Chem. Mater.* **1999,** *11*, 1526.

(17) Kovtyukhova, N.; Ollivier, P. J.; Chizhik, S.; Dubravin, A.; Buzaneva, E.; Gorchinskiy, A.; Marchenko, A.; Smirnova, N. *Thin Solid Films* **1999**, *337,* 166.

(18) Kovtyukhova, N. I.; Gorchinskiy, A. D.; Waraksa, C. C. *Mater. Sci. Eng.* **2000,** *B69,70*, 424.

(19) Kleinfeld, E. R.; Ferguson, G. S. *Science* **1994**, *265*, 370.

(20) Kovtyukhova, N.; Ollivier, P.; Martin, B.; Mallouk, T.; Buzaneva, E.; Gorchinskiy, A. *Chem. Mater.* **1999**, *11*, 771.

(21) Schmitt, J.; Decher, G.; Dressick, W.; Brandow, S. L.; Geer; R. E.; Shashidhar, R.; Calvert, J. M. *Adv. Mater.* **1997**, *9*, 61.

(22) Feldheim, D. L.; Grabar, K. C.; Natan, M. J.; Mallouk, T. E. *J. Am. Chem. Soc.* **1996**, *118*, 7640.

(23) (a) Cassagneau, T.; Fendler, J. H.; Mallouk, T. E. *Langmuir* **2000**, *16*, 241. (b) Cassagneau, T.; Mallouk, T. E.; Fendler, J. H. *J. Am. Chem. Soc.* **1998**, *120*, 7848.

(24) Gao, M.; Richter, B.; Kirstein, S.; Mohwald, H. *J. Phys. Chem.* **1998**, *102*, 4096.

(25) (a) Kaschak, D. M.; Mallouk, T. E. *J. Am. Chem. Soc.* **1996**, *118*, 4222. (b) Kaschak, D. M.; Lean, J. T.; Waraksa, C. C.; Saupe, G.; Usami, H.; Mallouk, T. E. *J. Am. Chem. Soc.* **1999**, *121*, 3435.

(26) Cepak, V. M.; Hulteen, J. C.; Che, G.; Jirage, K. B.; Lakshmi, B. B.; Fisher, E. R.; Martin, C. R. *Chem. Mater.* **1997**, *9*, 1065.

(27) Yu, J. S.; Kim, J. Y.; Lee, S.; Mbindyo, J. K. N.; Martin, B. R.; Mallouk, T. E. *J. Chem. Soc., Chem. Commun.* **2000**, 2445.

(28) Spanhel, L.; Anderson, M. A. *J. Am. Chem. Soc.* **1991**, *113*, 2826−2833.

(29) Chiang, J. B.; MacDiarmid, A. G. *Synth. Met.* **1986**, *13*, 193.

(30) Mallory, G. O., Hajdu, J. B., Eds. *Electroless Plating: Fundamentals and Applications*; American Electroplaters and Surface Finishers Society: Orlando, FL, 1990.

(31) Smith, P. A.; Nordquist, C. D.; Jackson, T. N.; Mayer, T. S.; Martin, J.B.; Mbindyo, R.; Mallouk, T. E. *Appl. Phys. Lett.* **2000**, *77*, 1399.

(32) Yokoyama, T.; Matsukado, Y.; Ichida, A.; Motomura, Y.; Watanabe, K.; Izawa, E. *J. Colloid Interface Sci.* **2001**, *233*, 112.